Published in final edited form as:
J Comp Neurol. 2012 February 15; 520(3): 620–632. doi:10.1002/cne.22755.

Sacral Neural Crest-Derived Cells Enter the Aganglionic Colon of *Ednrb*$^{-/-}$ Mice Along Extrinsic Nerve Fibers

Christopher S. Erickson[1], **Ismail Zaitoun**[1], **Kathryn M. Haberman**[1], **Ankush Gosain**[2], **Noah R. Druckenbrod**[3], and **Miles L. Epstein**[1,*]

[1]Department of Neurosciences, University of Wisconsin School of Medicine and Public Health, Madison, Wisconsin 53706

[2]Department of Surgery, University of Wisconsin School of Medicine and Public Health, Madison, Wisconsin 53706

[3]Department of Neurobiology, Harvard Medical School, Boston, Massachusetts 02115

Abstract

Both vagal and sacral neural crest cells contribute to the enteric nervous system in the hindgut. Because it is difficult to visualize sacral crest cells independently of vagal crest, the nature and extent of the sacral crest contribution to the enteric nervous system are not well established in rodents. To overcome this problem we generated mice in which only the fluorescent protein-labeled sacral crest are present in the terminal colon. We found that sacral crest cells were associated with extrinsic nerve fibers. We investigated the source, time of appearance, and characteristics of the extrinsic nerve fibers found in the aganglionic colon. We observed that the pelvic ganglion neurons contributed a number of extrinsic fibers that travel within the hindgut between circular and longitudinal muscles and within the submucosa and serosa. Sacral crest-derived cells along these fibers diminished in number from fetal to post-natal stages. A small number of sacral crest-derived cells were found between the muscle layers and expressed the neuronal marker Hu. We conclude that sacral crest cells enter the hindgut by advancing on extrinsic fibers and, in aganglionic preparations, they form a small number of neurons at sites normally occupied by myenteric ganglia. We also examined the colons of ganglionated preparations and found sacral crest-derived cells associated with both extrinsic nerve fibers and nascent ganglia. Extrinsic nerve fibers serve as a route of entry for both rodent and avian sacral crest into the hindgut.

INDEXING TERMS

Hirschsprung's disease; sacral neural crest; endothelin receptor b; *Ednrb*; enteric; aganglionic colon; megacolon

The rhombocephalic (vagal) neural crest is the major source of progenitors for the enteric nervous system (ENS). However, sacral neural crest-derived cells (SNCCs) also contribute

*CORRESPONDENCE TO: Miles L. Epstein, Department of Neurosciences, University of Wisconsin School of Medicine and Public Health, 1300 University Ave., Madison, WI 53706. mepstein@wisc.edu.

NOTE ADDED IN PROOF

Sacral crest advance on extrinsic fibers in wildtype mice, a finding similar to ours in *Ednrb*$^{-/-}$ and *Ednrb*$^{+/-}$ mice. Wang, X et al. 2011., Gastroenterology 141:992–1002.

Additional Supporting Information may be found in the online version of this article.

cells to the mature ENS in the colon (Burns and Le Douarin, 1998). Because of their close apposition to the hindgut, SNCCs have been viewed as a potential source of neuronal precursors to colonize the hindgut in Hirschsprung's disease (HSCR), a condition that results when the vagal neural crest cells fail to enter and form ganglia in the terminal portion of the hindgut.

Most of our information about the sacral neural crest comes from studies carried out in avian systems. In the avian gut, the sacral crest forms the pelvic plexus and the ganglionated Nerve of Remak (NoR) located in the dorsal mesentery of the hindgut and midgut. This nerve serves as both a source and pathway for sacral crest cells to enter the intestine and form enteric neurons (Burns and Le Douarin, 1998). In mice, sacral neural crest cells emigrate from the neural tube toward the pelvic viscera at embryonic day (E)11.5 and aggregate into nascent pelvic ganglia (PG) found ventrolateral to the hindgut at E14.5–E15 (Anderson et al., 2006). Although the pelvic ganglion and the NoR extend fibers and provide cells to the avian colon, the nature and extent of the contribution by sacral crest to the rodent ENS is less certain. Using DBH-lacZ mice, Kapur (2000) found a small number of SNCCs in the mouse colon at E13.5. At a similar age Druckenbrod and Epstein (2005) visualized the rostral movement of fluorescent protein-labeled SNCCs in the distal colon until they were obscured by vagal neural crest-derived cells (VNCCs) migrating aborally.

It has been difficult to visualize the contribution of SNCCs into the rodent hindgut because they are obscured by the presence of the VNCCs. SNCCs move from the nascent pelvic ganglion to the hindgut at around E13, the same time as the vagal crest colonizes the most caudal hindgut. To circumvent this problem our strategy was to use a mouse model of HSCR, one lacking the endothelin receptor B ($Ednrb^{-/-}$) in crest-derived cells. Such a preparation lacks VNCCs in the terminal colon and thus permits the visualization of the SNCCs.

MATERIALS AND METHODS

Animals

We generated mice in which exon 3 of the endothelin receptor B gene (*Ednrb*) was flanked by *loxP* sites. A floxed *Ednrb* targeting vector included exons 3–7 was created from a 129/SvJ BAC clone containing *Ednrb* in which the 5′ homology arm contained the terminal 3′ 2.2 kb portion of intron 2. A floxed neocassette was also attached to the 3′ end of intron 2 and a third *loxP* site was introduced into the 5′ end of intron 3 so that exon 3 was enclosed within the *loxP* sites. Constructs were introduced into SV/129 R1 embryonic stem cells; positive clones were identified and injected into C57BL/6 blastocysts to generate a founder line, called $Ednrb^{flex\ 3/+}$ mice. These were mated with $Tg^{Wnt1\text{-}Cre}$ *mice* (Danielian et al., 1997) to produce $Tg^{Wnt1\text{-}Cre/+}$ $Ednrb^{flex3/+}$ mice. $Ednrb^{flex3/flex3}$ mice were also bred with mice containing $Rosa26^{YFPStop/YFPStop}$ to generate $Rosa26^{YFPStop/YFPStop}$ $Ednrb^{flex3/flex3}$ mice. Mating the $Tg^{Wnt1\text{-}Cre/+}$ $Ednrb^{flex3/+}$ mice with $Rosa26^{YFPStop/YFPStop}$ $Ednrb^{flex3/flex3}$ mice resulted in deletion of exon 3 and the absence of a functional protein in neural crest cells (NCC). This was confirmed by western blot analysis (Druckenbrod et al., 2008). From the above mating about 50% of fetuses and animals expressed yellow fluorescent protein (YFP)-positive NCCs. Of these YFP+ preparations about half either lacked *Ednrb,* $Ednrb^{-/-}$, or contained one functional *Ednrb* allele (Druckenbrod et al., 2008; Druckenbrod and Epstein, 2009). $Ednrb^{-/-}$ animals can be recognized by the absence of YFP+ NCC in their distal colon. The $Ednrb^{flex3/flex3}$ mice are available from Jackson Laboratories (Bar Harbor, ME; Stock no. 009063). Fetuses were harvested from pregnant females that were killed by cervical dislocation after treatment with isoflurane. The embryo's phenotype was identified by observing the most distal position of the YFP+ VNCCs in the gut (Druckenbrod and Epstein, 2009); the most distal VNCCs cells in the $Ednrb^{+/-}$ preparations were more aboral

than the most distal cells in the *Ednrb*$^{-/-}$ mice. To obtain expression of β-galactosidase, *Tg*$^{Wnt1\text{-}Cre/+}$*Ednrb*$^{flex3/+}$ mice were bred to *Rosa26*$^{LacZ\ Stop/LacZ\ Stop}$ Ednrb$^{flex3/flex3}$ mice. The mice were housed in a nonsterile environment. All procedures were approved by the University of Wisconsin Animal Care Committee.

Tissue preparation

The entire gut was removed, opened (postnatal only), and pinned down mucosa side up in sylgard dishes. The gut lumen was washed and the gut was placed in 4% para-formaldehyde for fixation at room temperature for 4–6 hours or at 4°C overnight. Following fixation the preparation was washed in phosphate-buffered saline (PBS, pH 7.4). For whole-mount preparations the mucosa and sub-mucosa was removed from the fixed tissue. The detection of β-galactosidase was done by staining the postnatal gut overnight at room temperature using the standard staining solution (5 mM potassium ferricyanide, 5 mM potassium ferrocyanide, 2 mM $MgCl_2$, 0.4% X-gal in PBS). The tissue was then rinsed twice in PBS and postfixed in 4% formaldehyde. Frozen sections were prepared from tissue placed in 15% sucrose for 15 minutes, then a mixture of 50% OCT: 50% solution of 15% sucrose for 2–6 hours, and finally into 100% OCT overnight. Tissue was then frozen on dry ice and sectioned on a cryostat at a thickness of 11 μm.

Immunohistochemistry and image analysis

Fixed whole-mount tissue and cross sections were treated with 0.1–1.0% Triton X-100 for 4–6 hours at room temperature or overnight at 4°C, washed in PBS, incubated with primary antibodies (Table 1) for 4–6 hours at room temperature or overnight at 4°C, washed in PBS, and then stained with corresponding secondary antibodies (Table 2) for 4–6 hours at room temperature or overnight at 4°C. The immunostained preparations were visualized using a Nikon inverted microscope equipped with a Photometrics Cool-SNAP camera or with a Bio-Rad (Hercules, CA) MRC 1024 confocal microscope. Images were captured, processed, and analyzed with Metamorph (Molecular Devices, Palo Alto, CA). The images were edited and some enhanced by adjusting brightness and contrast using the photo editing software Paint.NET (dotPDN LLC).

Antibody characterization

The list of primary antibodies used is shown in Table 1.

The mouse monoclonal class III β-tubulin antibody, produced by Dr. A. Frankfurter, was made using the peptide EAQGPK corresponding to the C-terminus of β III tubulin. The production, purification, and characterization of this antibody have been described previously (Lee et al., 1990).

The neurofilament (NF) antibody is a rabbit polyclonal (Chemicon, Temecula, CA; no. AB1987) prepared against a recombinant protein containing the C-terminal 168 amino acids of rat NF-M fused to *E. coli* Trp-E (manufacturer's information). On western blots of chicken brain extract the antibody stains a single band at 145 kDa molecular weight and the antibody strongly recognizes NF-M but not NF-H in the brain of cow, pig, and chicken by immunoblotting (Harris et al., 1991).

The tyrosine hydroxylase (TH) monoclonal mouse antibody (IncStar, Stillwater, MN; no. 22941) was raised against TH purified from rat PC12 cells. This antibody is believed to have wide species crossreactivity (manufacturer's datasheet) and the antiserum specifically labels rainbow trout TH in western blot analysis of brain extract and transfected COS-1 cells (Linard et al., 1998).

The chicken polyclonal TH antiserum (Aves Labs, Tigard, OR; no. TYH) is a mixture of two different antipeptide antibodies. One was generated against a peptide near the N-terminus and one near the C-terminus of TH. The N-terminal peptide is RRQ SLI EDA RKE RE (corresponding to residues 68–81 of the human gene product [P07101] and 37–50 of the mouse gene product [P24529]). The C-terminal peptide is SDA KDK LR[N/S] YAS RIQ R (corresponding to residues 469–484 of the human gene product and 439–454 of the mouse gene product). Note that the arginine at position 9 of this peptide corresponds to the mouse gene product, and the serine corresponds to the human gene product (manufacturer's information).

The polyclonal human anti-Hu was collected from a patient. Such serum is usually obtained from patients suffering from paraneoplastic syndromes. This antiserum recognized a single band of 41 kDa on western blots of extracts of chicken brain. Hu belongs to a family of neuron-restricted RNA binding proteins related to the *Drosophila* RNA binding proteins Elav and Sex-lethal (Fairman et al., 1995).

The rabbit polyclonal nitric oxide synthase (NOS) antiserum (BD Transduction Laboratories, San Diego, CA; N31030/L15) was raised against residues 1095–1290 of human nNOS, corresponding to residues 1091–1286 of rat nNOS with five amino acid substitutions, which span parts of the FAD and NADPH binding motifs (manufacturer's datasheet).

The sheep polyclonal NOS antiserum, a generous gift from P.C. Emson, was raised against recombinant rat NOS. This antiserum recognizes neuronal NOS by western blotting and the immunoreactivity is abolished by absorption of the K205 antiserum with recombinant neuronal NOS protein (Herbison et al., 1996; Morona and González, 2008).

The rabbit polyclonal vasoactive intestinal polypeptide (VIP) antiserum was produced by conjugating porcine VIP to bovine thyroglobulin with 1-ethyl-3-(3-dimethylaminopropyl)-carbodimide. Incubation of antisera with VIP abolished immunostaining (Epstein and Paulsen, 1991).

The rabbit polyclonal green fluorescent protein (GFP) antiserum (Abcam, Cambridge, MA; AB290) recognizes the expected (27 kDa) band on western blot of GFP-positive transgenic mouse brain (manufacturer's datasheet). The chicken polyclonal GFP antiserum (Aves Labs, GFP-1020) was analyzed by western blot analysis and immunohistochemistry using transgenic mice expressing the GFP gene product (manufacturer's datasheet). GFP immunostaining was not detected in the gut of wildtype mice.

DiI labeling

Colons with the pelvic ganglia attached were removed from postnatal YFP+ *Ednrb*$^{-/-}$ mice and the nerve fibers were visualized using a Nikon fluorescent stereoscope. A DiI C^{18} crystal (Invitrogen, La Jolla, CA; D-3911) was placed on the targeted fiber and allowed to adhere for 30 seconds. The tissue with the attached DiI crystal was then submerged in culture media (Dulbecco's modified Eagle's medium [DMEM]/F12 containing penicillin, streptomycin, and amphothericin, pH 7.4) and incubated at 37°C for 2 days before fixation in 4% paraformaldehyde.

RNA extraction and quantitative real-time polymerase chain reaction (PCR)

Colons were harvested from E16.5 *Ednrb*$^{-/-}$ and *Ednrb*$^{+/-}$ mice, a stage when a number of SNCCs are present in the colon. The colon was divided into three distinct pieces, the wavefront (2–4 mm): defined as the most caudal continuous strands of YFP+ cells, the colonized region (4–8 mm): the remaining section of colonized proximal colon, and

aganglionic colon (*Ednrb*$^{-/-}$ only, 5–10 mm): the remaining section of distal colon not colonized with any vagal ENCCs. The pelvic ganglia were detached from both *Ednrb*$^{-/-}$ and *Ednrb*$^{+/-}$ colons. These tissue samples were placed in RNAlater (Sigma-Aldrich, St. Louis, MO) and kept at −20°C until extraction of RNA. RNA was isolated using the RNeasy Mini Kit (Qiagen, Chatsworth, CA) and quantified using a NanoDrop ND-1000 spectrophotometer (Thermo Fisher Scientific, Pittsburgh, PA). cDNA was synthesized with equal amounts of RNA from different samples using a High Capacity cDNA Reverse Transcription Kit (Applied Biosystems, Foster City, CA). Equal amounts of cDNA were added to quantitative real-time PCR reactions that were performed on CFX96 instrument (Bio-Rad) using SYBR Green chemistry (Bio-Rad). Since the sequences of EGFP and YFP are similar, the EGFP primers are able to detect YFP. The *Ret* and YFP(EGFP) primers were as follows: *Ret* forward 5′-CCAGCATCTCTATGGCGTCT-3′ and reverse 5′-GCGGATCCAGTCATTCTCAT-3′; EGFP forward 5′-GCA GAAGAACGGCATCAAGGT-3′ and reverse 5′-ACGAACTC CAGCAGGACCATG-3′. EGFP was used as an internal control; the *Ret* values were normalized to the EGFP values. The fold change in target gene expression was measured between *Ednrb*$^{-/-}$ and *Ednrb*$^{+/-}$ according to the comparative C(T) method (Schmittgen and Livak, 2008). Data are presented as mean ± standard error from nine separate experiments; each experiment contained tissue from 2–3 fetuses.

RESULTS

Our mating scheme (Druckenbrod et al., 2008) results in litters in which about 50% of the pups express the YFP and half of these YFP+ preparations express one functional *Ednrb* allele (*Ednrb*$^{+/-}$) and the other half lack a functional *Ednrb* allele (*Ednrb*$^{-/-}$). Such mice allow us to visualize easily the aganglionic regions of the gut. The aganglionic mice die at about postnatal day (P)30–35 from Hirschsprung's associated complications. One of the distinguishing characteristics of the aganglionic colon is the presence of a large number of thick nerve fascicles throughout the aganglionic region (Wedel et al., 2008). We found that SNCCs are located along nerve fibers that extend into the aganglionic colon and provide evidence that these fibers are a path for entry of SNCCs into the hindgut. We will first describe the appearance of these fibers and then focus on the properties of the SNCCs.

Nerve fibers

In the fetal *Ednrb*$^{-/-}$ colon, nerve fascicles are found throughout the aganglionic portion, while very few are apparent in the ganglionated *Ednrb*$^{+/-}$ colon (Fig. 1). Most fibers entering the gut appear to be spatially associated with the pelvic ganglion in these isolated preparations. In the *Ednrb*$^{+/-}$ preparation most fibers are positioned outside the colon. Most fibers projected aborally to the anus but a small number (2–4) projected a short distance, 5–12 mm, orally. The ganglia obscured the path of these fibers so their course was difficult to follow. The entire colon is colonized by E14 in *Ednrb*$^{+/-}$ fetuses, the same stage as in wildtype mice (Kapur, 2000). In contrast, the *Ednrb*$^{-/-}$ colon contains fibers throughout aganglionic regions both oral and aboral to the pelvic ganglion and these fibers appear to enter the colon near the pelvic ganglion. We examined *Ednrb*$^{-/-}$ fetuses and pups to determine the developmental timetable for the appearance of the fibers. Examination of null E15 fetuses indicates that nascent extrinsic fibers exit the pelvic ganglia primarily toward the rectum, although some begin to extend proximally (Fig. 2A,E). At E17 the colon has increased in size; the network of fibers is more extensive proximal to the pelvic ganglion (Fig. 2B). By P0–P1 the most proximal fibers have reached the ganglionic/aganglionic boundary and thick and thin fibers are apparent (Fig. 2C,F). The sacral fiber network in the P7 gut contains a few thick fibers and many smaller fibers that ramify throughout the

aganglionic colon; some of the fibers advance into and beyond the hypoganglionic region (Fig. 2D). This network appears to be the same at P23 as at P7 (data not shown).

The fibers in the null colons varied in size and in their position, a finding that suggested they might travel at different depths within the gut wall. In order to determine which layer(s) contained these extrinsic fibers we sectioned the gut from *Ednrb*$^{+/-}$ and *Ednrb*$^{-/-}$ mice (Fig. 3). In the *Ednrb*$^{-/-}$ gut the large fascicles of fibers were mostly confined to the region between the circular and longitudinal muscle, normally occupied by myenteric ganglia (Fig. 3C,D), while the small bundles of fibers occasionally are present in the submucosa (Fig. 6F,H) and serosa (Fig. 3C). When fibers in the *Ednrb*$^{-/-}$ extend into the hypoganglionic region (Fig. 7B,C; Supporting Fig. S2B), populated by the vagal crest-derived ganglia, small fascicles were found superficial to the longitudinal muscle, while the large sacral fascicles continued between the muscle layers and extended orally. The origin of the small fascicles in the serosa could be either the sacral axons and /or the vagally derived intrinsic neurons in the hypoganglionic region. Figure 7D is a diagram showing the arrangement of the small fascicles. In the *Ednrb*$^{+/-}$ colon sacral-derived fibers are observed in the serosa superficial to the longitudinal muscle for most of their length and penetrated the longitudinal muscle to terminate in the region of myenteric ganglia (Fig. 3A,B; Supporting Fig. S1).

Since many fibers projected from the pelvic ganglion, we investigated whether the fibers found in the aganglionic colon arose from neurons in the pelvic ganglion. We placed pieces of DiI crystals on fibers in P19 and P29 aganglionic colons that were then cultured for 2–3 days and fixed. As shown in Figure 4, DiI appears in some pelvic ganglion neurons and nerve fibers projecting into the aganglionic colon. This result indicates that some of the fibers originate from neurons in the pelvic ganglion. To see if the sacral contribution was similar in *Ednrb*$^{+/-}$ animals, DiI was also used to label fibers near the pelvic ganglia (Fig. S1). The fibers appear to be associated with the myenteric ganglia but do not appear to extend aborally a great distance after entering the muscle layers.

The pelvic ganglia produce a number of neurotransmitter-associated markers including TH and VIP (Wanigasekara et al., 2003). We found many sacral fibers in the *Ednrb*$^{-/-}$ colon were immunoreactive (IR) for TH (Fig. 5), a few were IR for VIP, and none were IR for nitric oxide synthase (data not shown). The sacral fibers also contained βIII-tubulin and neurofilament protein-IR (Fig. 6A,F).

Sacral neural crest-derived cells

The pelvic ganglia arise from SNCCs (Kapur, 2000; Anderson et al., 2006). Because we observed some of the extrinsic fibers in the aganglionic region to originate from this ganglion, we further examined these fibers for the presence of SNCCs. We found cells clustered along nerve fibers in both fetal and postnatal preparations. At E14.5 individual YFP+ cells appeared at intervals along βIII-tubulin-IR fibers that leave the pelvic ganglion (Fig. 6A). At E15 many YFP+ cells are spaced along fibers as observed in whole mounts of E15 distal colon (Fig. 6B). Sections of E15 distal colon indicate that the cells are associated with fibers located between the longitudinal and circular muscle layers (Fig. 6C,D). At E17 the majority of cells are found near the pelvic ganglia and at the most oral position of fibers, with a few in between. Some of the cells in the colon near the pelvic ganglia become Hu+ at this age (data not shown). In postnatal colon more cells become Hu+ (Fig. 6E; S2A), with most appearing close to the pelvic ganglion, some in the most proximal fiber locations on the colon, and a few in between. Consistent with the position of the extrinsic fibers between the circular and longitudinal muscle, the Hu+ cells are found in the site normally occupied by myenteric ganglia (Fig. 6F–H). Usually individual Hu+ cells are found but occasionally a cluster of 2–4 cells occurs (data not shown).

One of the characteristics of VNCCs is their expression of TH between E10–12 (Baetge and Gershon, 1989). To determine whether the SNCCs might share this property and express TH, we immunostained preparations at E13.5–16.5, when SNCCs appear in the colon, for both TH and YFP. In each of the three *Ednrb*$^{-/-}$ and three *Ednrb*$^{+/-}$ E16.5 preparations examined, ≈30–40 TH-IR cells were found along nerve fibers entering the most distal colon (Fig. 7A,E,F). In the *Ednrb*$^{+/-}$ preparations we found TH+ cells that appeared to be incorporated into a myenteric ganglion (Fig. 7E,F). Sacral cells and fibers reach the vagal ganglia in a path diagramed in Figure 7G. Our impression is that the number of TH+ cells was not different between the two genotypes. The presence of the TH+ cells is consistent with the identification of the YFP+ cells on the extrinsic fibers being SNCCs. Together these data show that SNCCs invade both the aganglionic and the ganglionated hindgut. In both genotypes the number of TH+ cells is small; even in the absence of ganglia the SNCCs fail to expand sufficiently to form ganglia.

Why do SNCCs fail to colonize the colon? One explanation comes from experiments indicating that the expression of *Ret*, the GDNF receptor that controls many activities of enteric neural crest-derived cells, is reduced in SNCCs compared to VNCCs (Delalande et al., 2008). We used a different technique, real-time PCR, to measure whether differences in *Ret* expression occurred between VNCCs and SNCCs, both of which lack EDNRB, in the same piece of colon. Each crest cell receives only one copy of the YFP gene, and we assume but do not know whether the SNCCs and VNCCs have similar levels of YFP expression. We used the values of YFP expression as a measure of the number of YFP cells to calculate the value of *Ret* expression. We found that the RET mRNA levels of VNCCs at the vagal wavefront relative to the SNCCs was 2.87 ± 0.74 in *Ednrb*$^{-/-}$ E16.5 tissues. These data indicate that SNCCs express less *Ret* than VNCCs, a result consistent with a reduced capacity to proliferate (Pachnis et al., 1993; Gianino et al., 2003; Delalande et al., 2008).

DISCUSSION

By using a mouse model of HSCR in which the distal colon remains uncolonized, we are able to view only SNCCs and study their contribution to the terminal portion of the colon. We find the projections from the pelvic ganglion appear in the colon at E13.5, become abundant in the aganglionic region, and then extend into the hypoganglionic region. Retrograde labeling revealed that some fibers arose from neurons in the pelvic ganglion. Unlike the superficially located fibers in the *Ednrb*$^{+/-}$, most fibers traveled between the circular and longitudinal muscles in the aganglionic colon of *Ednrb*$^{-/-}$ mice. SNCCs are found alongside or within these fibers in *Ednrb*$^{-/-}$ fetal and post-natal colons and some differentiated into Hu+ neurons found between the longitudinal and circular muscle layers. Some SNCCs express TH and TH+ SNCCs are found in a few vagal-derived *Ednrb*$^{+/-}$ ganglia. We hypothesize that SNCCs move along nerve fibers from the pelvic ganglia to enter the terminal portion of aganglionic and ganglionated colon and some form neurons.

Sacral cell colonization of the mouse aganglionic colon and the bird are similar

The entry path of rodent SNCCs into the hindgut is homologous to that described for avian SNCCs entering the colon. In birds, sacral crest form the ganglionated NoR that extends from the cloaca to the initial part of the jejunum. Neurons in the NoR project processes into the gut and subsequently sacral crest move along these fibers to enter the bowel and contribute to nascent myenteric ganglia (Burns and Le Douarin, 1998). The entry of the fibers from the NoR into the colon occurs around E8, the same time as the chemorepellent Sema3A disappears from the outer muscular layers (Shepherd and Raper, 1999), while the SNCCs enter around E10 (Burns and Le Douarin, 1998). Consistent with these avian studies, Anderson et al. (2007) observed that a small number of SNCCs and fibers made a premature advance into Sema3a null mouse E13.5 hindgut. Our data indicate that sacral

crest migrate on fibers of the pelvic ganglion to enter the rodent colon, an arrangement similar to the bird. Another similarity is that both NoR and the pelvic ganglion share the property of having both sympathetic and parasympathetic neurons (Teillet, 1978; Keast, 1995).

Although the route of entry of rodent sacral crest cells into the colon has been unclear, SNCCs are found in a number of aganglionic preparations: near the anal region in the null *Ret* (Durbec et al., 1996), within the wall of the colon in the null GFRa1 mouse (Cacalano et al., 1998), and in the avian hindgut after ablation of the vagal neural crest (Burns et al., 2000). Anderson et al. (2006) described the presence of sacral crest-derived Hu+ cells along nerve fibers in the fetal colon of null *Ret* preparations. They found that the number of Hu+ cells increased with fetal age, did not colonize beyond 1.25 mm of the colon terminus, and showed a reduced expression of NOS compared to $Ret^{+/-}$ preparations that contain both VNCCs and SNCCs. Using a preparation in which *Ret* is functional, we have expanded on their observations to describe the presence of the Hu+ neurons in the gut wall in postnatal preparations. These data show that SNCCs can enter a hindgut lacking VNCCs and embed between the circular and longitudinal muscle to form Hu+ neurons along the length of an aganglionic preparation. These results suggest that the colon of $Ednrb^{-/-}$ mice permits the entry of SNCCs. In a previous report (Druckenbrod and Epstein, 2009) we observed that VNCCs did not enter the proximal colon after E14.5. The reason for this difference is not clear but could be dissimilar properties of the vagal and sacral crest cells and/or the different regions of the colon involved.

While our data do not provide any information on the movement of the SNCCs, we hypothesize that the SNCCs move along the fibers. This arrangement of neural progenitors along nerve fibers has also been seen in other preparations: TH+-positive VNCCs are found along the vagus nerve in the E10.5 mouse and use it as a pathway into the bowel (Baetge and Gershon, 1989; Baetge et al., 1990), SNCCs enter the hindgut along fibers projecting from NoR in the E10.5 avian embryo (Burns and Le Douarin, 1998), and Hu+ cells are found in the E7.5 chick vagus (Fairman et al., 1985) and on fibers from NoR entering the distal colon (Conner et al., 2003).

TH is expressed in some SNCCs

Since TH expression is detected in VNCCs at E10–12, which never take on a sympathetic fate (Baetge and Gershon, 1989), we wished to determine whether it is also found in SNCCs. We immunostained the YFP-labeled ENS progenitors in the hindgut. We observed a few TH+ cells among the nascent YFP+ ganglia in the E16.5 $Ednrb^{+/-}$ colon and associated with nerve fibers entering the hindgut in $Ednrb^{+/-}$ and $Ednrb^{-/-}$ colons. This small number of TH+ cells is similar to the proportion of TH+ cells we observed in the VNCCs population in the E11.5 mouse foregut (data not shown). It is possible that these TH + cells are derived from SNCCs that migrated from the pelvic ganglion.

Sacral projections in the aganglionic colon

Investigators have previously studied the sources of extrinsic neural fibers in the ganglionated hindgut, especially the pelvic ganglion that has been characterized extensively by Keast and colleagues (reviewed in Keast, 2006). In the rat the processes of pelvic ganglion neurons terminate via the rectal nerves mostly in the myenteric plexus but not in the mucosa or submucosa (Luckensmeyer and Keast, 1998a). In addition to the two pelvic ganglia, sacral-derived adventitial ganglia are present in the rectum near the anus and project to the internal anal sphincter and adjacent circular muscle (Luckensmeyer and Keast, 1998b).

Much of our information about the changes resulting from the absence of ganglia comes from studies of the null lethal-spotted (*ls*) mouse. The *ls* mutant, which lacks endothelin-3, a ligand for EDNRB, shows a phenotype similar to our null EDNRB preparation. Endothelin-3 is expressed by the mesenchymal cells, while EDNRB is found in both mesenchymal and neural crest derived cells along the developing gut (Wu et al., 1999; Barlow et al., 2003). In the *ls* mouse nerve fibers are hypertrophied and are densely arranged in the submucosa, where they extend orally to the hypoganglionic portion of the colon (Payette et al., 1987). These investigators also reported an increase in both the number of fiber bundles in the adventitia located near the anus and the number of adventitial ganglia of unusual morphology within these fiber bundles. The adventitial ganglia showed an unusual morphology in that they were situated on the serosal side of circular muscle at sites lacking longitudinal muscle. Payette et al. (1987) also reported that nerve fibers near the anus of both control and null *ls* mice had cell bodies located in L6 to S2 dorsal root ganglia, the inferior myenteric ganglion, and the ventral portion of L6-S1 motorcolumns. In the *Ednrb*$^{-/-}$ mouse, which has an aganglionic region of about 20 mm, in contrast to the 2 mm in the null *ls* mouse, we found that some fibers arose from neurons in the pelvic ganglion. Furthermore, our observations indicate a difference between the route taken by these fibers in aganglionic and ganglionated colon. Whereas the fibers in the colon containing ganglia remained outside the gut wall until terminating, those in the aganglionic colon traveled within the muscle wall. In the *Ednrb*$^{-/-}$ we observed fibers in the submucosa, in the space between the circular and longitudinal muscles (the location normally occupied by myenteric neurons), and occasionally in the circular muscle. Our observation of fibers in the submucoa is consistent with Payette's report in the *ls* mouse and fibers in the myenteric region are consistent with that of Luckensmeyer and Keast in the control mouse (1998a). The difference in paths taken in ganglionic compared to aganglionic colon may reflect the presence of ganglia producing a repellant that prevents a long fiber trajectory but permits entry of just the terminal process.

Why don't more sacral cells colonize the colon?

The number of sacral cells is small compared to the number of vagal crest in the same *Ednrb*$^{-/-}$ preparation. In the postnatal animals, the YFP+ sacral crest were less dense than in the fetus. Some expressed the neuronal marker Hu, and were found as individual cells or small clusters along the entire portion of the aganglionic gut. Previous work suggests that the small number of sacral crest cells is attributed to the reduced level of *Ret* found in avian sacral compared to vagal ENCCs (Burns et al., 2002; Delalande et al., 2008). Our analysis of *Ret* in *Ednrb*$^{-/-}$ sacral and vagal-derived crest cells supports their finding of a reduced expression of *Ret* in SNCCs, although the experiments were substantially different. Using real-time PCR, we analyzed intact tissue removed from a mouse preparation that lacked EDNRB in neural crest cells only. Our values of mRNA were normalized to YFP expression and thus controlled for the number of crest cells in the sample. In contrast Delalande et al. (2008) obtained a value of 4.27 after measuring differences in cDNA binding to an array using avian crest cells that migrated off the neural tube and were cultured for 18 hours.

In summary, our findings indicate that SNCCs invade the aganglionic colon along nerve fibers, some of which arise from the pelvic ganglia, and form a small number of neurons at the site occupied by myenteric ganglia. The SNCCs do not proliferate in sufficient numbers to form ganglia; this failure may be related to reduced levels of the RET receptor. However, our observations are limited to sacral crest cells that are subject to the same defects that can affect vagal crest colonization in HSCR so that the pattern of colonization in nulls may be different from that in *Ednrb*$^{+/-}$ or wildtype mice. Further investigations are needed to determine whether the same pattern occurs in the ganglionated colon.

Supplementary Material

Refer to Web version on PubMed Central for supplementary material.

Acknowledgments

Grant sponsor: National Institutes of Health; Grant number: R01-DK081634.

We thank P.C. Emson for the gift of sheep anti-NOS antibody and the W.M. Keck Laboratory for Biological Imaging and Lance Rodenkirch for the use of their confocal.

This article is dedicated to the memory of Jeffery W. Walker (1954–2010), esteemed colleague who left us much too soon.

LITERATURE CITED

Anderson RB, Stewart AL, Young HM. Phenotypes of neural-crest-derived cells in vagal and sacral pathways. Cell Tissue Res. 2006; 323:11–25. [PubMed: 16133146]

Anderson RB, Bergner AJ, Taniguchi M, Fujisawa H, Forrai A, Robb L, Young HM. Effects of different regions of the developing gut on the migration of enteric neural crest-derived cells: a role for Sema3A, but not Sema3F. Dev Biol. 2007; 305:287–299. [PubMed: 17362911]

Baetge G, Gershon MD. Transient catecholaminergic (TC) cells in the vagus nerves and bowel of fetal mice: relationship to the development of enteric neurons. Dev Biol. 1989; 132:189–211. [PubMed: 2563710]

Baetge G, Schneider KA, Gershon MD. Development and persistence of catecholaminergic neurons in cultured explants of fetal murine vagus nerves and bowel. Development. 1990; 110:689–701. [PubMed: 1982430]

Barlow A, de Graaff E, Pachnis V. Enteric nervous system progenitors are coordinately controlled by the G protein-coupled receptor EDNRB and the receptor tyrosine kinase RET. Neuron. 2003; 40:905–916. [PubMed: 14659090]

Burns AJ, Le Douarin NM. The sacral neural crest contributes neurons and glia to the post-umbilical gut: spatio-temporal analysis of the development of the enteric nervous system. Development. 1998; 125:4335–4347. [PubMed: 9753687]

Burns AJ, Champeval D, Le Douarin NM. Sacral neural crest cells colonise aganglionic hindgut in vivo but fail to compensate for lack of enteric ganglia. Dev Biol. 2000; 219:30–43. [PubMed: 10677253]

Burns AJ, Delalande JM, Le Douarin NM. In ovo transplantation of enteric nervous system precursors from vagal to sacral neural crest results in extensive hindgut colonisation. Development. 2002; 129:2785–2796. [PubMed: 12050129]

Cacalano G, Farinas I, Wang LC, Hagler K, Forgie A, Moore M, Armanini M, Phillips H, Ryan AM, Reichardt LF, Hynes M, Davies A, Rosenthal A. GFRalpha1 is an essential receptor component for GDNF in the developing nervous system and kidney. Neuron. 1998; 21:53–62. [PubMed: 9697851]

Conner PJ, Focke PJ, Noden DM, Epstein ML. Appearance of neurons and glia with respect to the wavefront during colonization of the avian gut by neural crest cells. Dev Dyn. 2003; 226:91–98. [PubMed: 12508228]

Delalande JM, Barlow AJ, Thomas AJ, Wallace AS, Thapar N, Erickson CA, Burns AJ. The receptor tyrosine kinase RET regulates hindgut colonization by sacral neural crest cells. Dev Biol. 2008; 313:279–292. [PubMed: 18031721]

Druckenbrod NR, Epstein ML. The pattern of neural crest advance in the cecum and colon. Dev Biol. 2005; 287:125–133. [PubMed: 16197939]

Druckenbrod NR, Epstein ML. Age-dependent changes in the gut environment restrict the invasion of the hindgut by enteric neural progenitors. Development. 2009; 136:3195–3203. [PubMed: 19700623]

Druckenbrod NR, Powers PA, Bartley CR, Walker JW, Epstein ML. Targeting of endothelin receptor-B to the neural crest. Genesis. 2008; 46:396–400. [PubMed: 18693272]

Durbec PL, Larsson-Blomberg LB, Schuchardt A, Costantini F, Pachnis V. Common origin and developmental dependence on c-ret of subsets of enteric and sympathetic neuroblasts. Development. 1996; 122:349–358. [PubMed: 8565847]

Epstein ML, Poulsen KT. Appearance of somatostatin and vasoactive intestinal peptide along the developing chicken gut. J Comp Neurol. 1991; 311:168–178. [PubMed: 1682349]

Fairman CL, Clagett-Dame M, Lennon VA, Epstein ML. Appearance of neurons in the developing chick gut. Dev Dyn. 1995; 204:192–201. [PubMed: 8589443]

Gianino S, Grider JR, Cresswell J, Enomoto H, Heuckeroth RO. GDNF availability determines enteric neuron number by controlling precursor proliferation. Development. 2003; 130:2187–2198. [PubMed: 12668632]

Harris J, Ayyub C, Shaw G. A molecular dissection of the carboxyterminal tails of the major neurofilament subunits NF-M and NF-H. J Neurosci Res. 1991; 30:47–62. [PubMed: 1724473]

Herbison AE, Simonian SX, Norris PJ, Emson PC. Relationship of neuronal nitric oxide synthase immunoreactivity to GnRH neurons in the ovariectomized and intact female rat. J Neuroendocrinol. 1996; 8:73–82. [PubMed: 8932739]

Kapur RP. Colonization of the murine hindgut by sacral crest-derived neural precursors: experimental support for an evolutionarily conserved model. Dev Biol. 2000; 227:146–155. [PubMed: 11076683]

Keast JR. Visualization and immunohistochemical characterization of sympathetic and parasympathetic neurons in the male rat major pelvic ganglion. Neuroscience. 1995; 66:655–662. [PubMed: 7644029]

Keast JR. Plasticity of pelvic autonomic ganglia and urogenital innervation. Int Rev Cytol. 2006; 248:141–208. [PubMed: 16487791]

Lee MK, Tuttle JB, Rebhun LI, Frankfurter A. The expression and posttranslational modification of a neuron-specific β-tubulin isotype during chick embryogenesis. Cell Motil Cytoskeleton. 1990; 17:118–132. [PubMed: 2257630]

Linard B, Pakdel F, Marmignon MH, Saligaut C. Cloning of a cDNA coding for active tyrosine hydroxylase in the rainbow trout (Oncorhynchus mykiss): comparison with other hydroxylases and enzymatic expression. J Neurochem. 1998; 71:920–928. [PubMed: 9721717]

Luckensmeyer GB, Keast JR. Projections of pelvic autonomic neurons within the lower bowel of the male rat: an anterograde labelling study. Neuroscience. 1998a; 84:263–280. [PubMed: 9522380]

Luckensmeyer GB, Keast JR. Characterisation of the adventitial rectal ganglia in the male rat by their immunohistochemical features and projections. J Comp Neurol. 1998b; 396:429–441. [PubMed: 9651003]

Morona R, González A. Calbindin-D28k and calretinin expression in the forebrain of anuran and urodele amphibians: further support for newly identified subdivisions. J Comp Neurol. 2008; 511:187–220. [PubMed: 18781620]

Pachnis V, Mankoo B, Costantini F. Expression of the c-ret proto-oncogene during mouse embryogenesis. Development. 1993; 119:1005–1017. [PubMed: 8306871]

Payette RF, Tennyson VM, Pham TD, Mawe GM, Pomeranz HD, Rothman TP, Gershon MD. Origin and morphology of nerve fibers in the aganglionic colon of the lethal spotted (ls/ls) mutant mouse. J Comp Neurol. 1987; 257:237–252. [PubMed: 3571527]

Schmittgen TD, Livak KJ. Analyzing real-time PCR data by the comparative C(T) method. Nat Protoc. 2008; 3:1101–1108. [PubMed: 18546601]

Shepherd IT, Raper JA. Collapsin-1/semaphorin D is a repellent for chick ganglion of Remak axons. Dev Biol. 1999; 212:42–53. [PubMed: 10419684]

Teillet MA. Evolution of the lumbo-sacral neural crest in the avian embryo: origin and differentiation of the ganglionated nerve of Remak studied in interspecific quail-chick chimera. Roux's Arch Dev Biol. 1978; 182:251–268.

Wanigasekara Y, Kepper ME, Keast JR. Immunohistochemical characterisation of pelvic autonomic ganglia in male mice. Cell Tissue Res. 2003; 311:175–185. [PubMed: 12596037]

Wedel, T.; Krammer, HJ.; Holschneider. Hirschsprung's disease and allied disorders. 3. 2008. Electron microscopic studies of Hirschsprung's disease; p. 221-228.

Wu JJ, Chen JX, Rothman TP, Gershon MD. Inhibition of in vitro enteric neuronal development by endothelin-3: mediation by endothelin B receptors. Development. 1999; 126:1161–1173. [PubMed: 10021336]

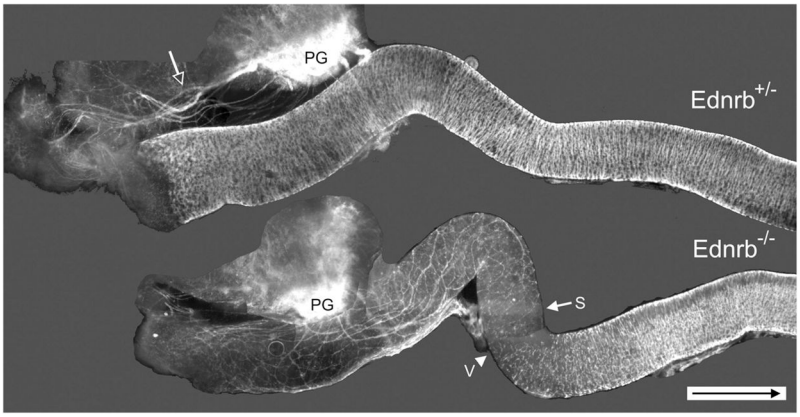

Figure 1.

Distribution of YFP expression in freshly isolated E16.5 *Ednrb*$^{+/-}$ and *Ednrb*$^{-/-}$ hindgut. In the *Ednrb*$^{+/-}$ colon the majority of nerve fibers (open arrow) radiate from the pelvic ganglia (PG) and travel outside the colon until reaching the anal region; the entire colon is occupied by ganglia shown as white lines. In comparison, most fibers enter the *Ednrb*$^{-/-}$ distal colon and project in oral and aboral directions. Arrow indicates the most oral position of sacral nerve fibers; arrowhead indicates the most aboral position of the vagal crest wavefront. The figure is a photomontage. Arrow inside scale bar indicates oral direction. Scale bar = 500 μm.

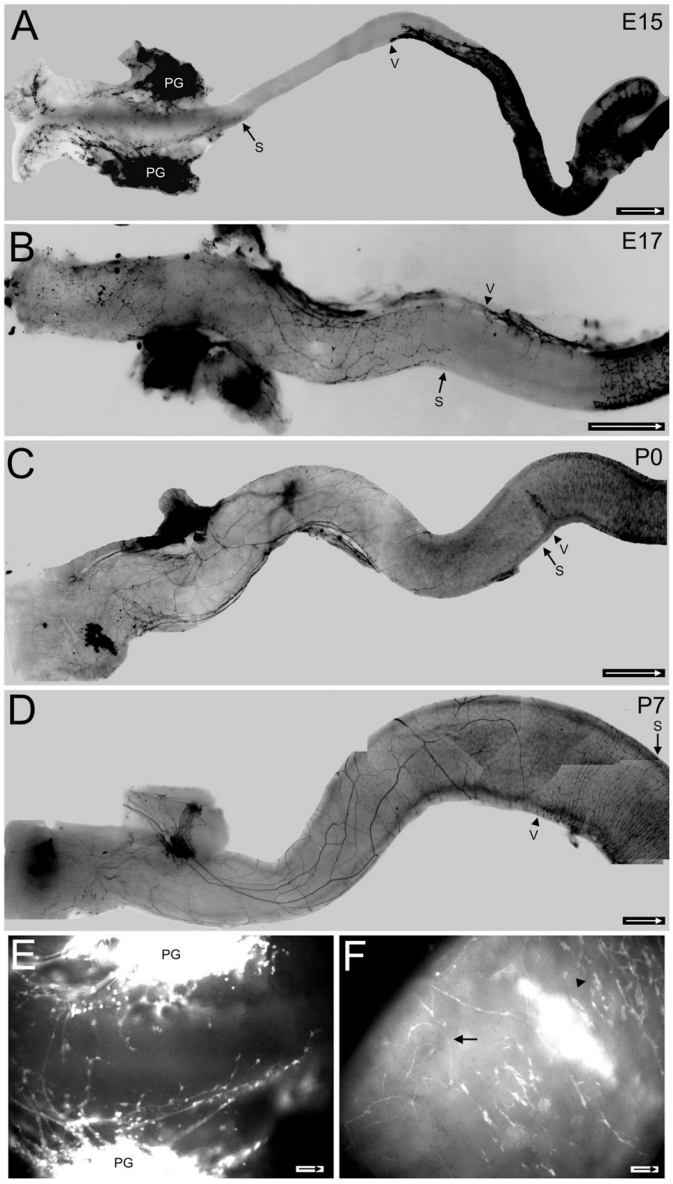

Figure 2.

Development of sacral fibers in freshly isolated *Ednrb*$^{-/-}$ colons. In A–D arrow indicates the most oral position of the sacral wavefront, arrowhead shows the most aboral position of the vagal wavefront. YFP signals are dark in A–D and light in E,F. **A**: At E15 processes from the pelvic ganglion project in oral and aboral directions. The vagal wavefront has moved into the midcolon and will not advance much further. **B**: At E17 nerve fibers have advanced orally and form a network of large and small processes. The vagal wavefront is found at the midcolon with the mesenteric strand extending aborally and from it crest cells will move laterally across the width of the colon. **C**: At birth (P0) the sacral nerve fibers have advanced to the site of the vagal wavefront. Note that the vagal wavefront contains many cells. **D**: At P7 large sacral fibers are apparent and some extend into the region occupied by the vagal crest-derived cells while smaller fibers extend extensive processes of varying sizes. The sacral fibers and vagal crest have also begun to intermingle at the midcolon. **E**: An enlargement of the terminal region of (A). Nerve fibers arise from pelvic ganglia (PG). Note

the enlarged swellings are sacral-derived neural crest cells along the nerve fibers. **F**: An enlargement of the midcolon where the sacral fibers (arrow) and vagal crest cell wavefront (arrowhead) meet in the P0 colon in (C). A–D are photomontages. Arrow inside scale bar indicates oral direction. Scale bars = 500 μm in A; 250 μm in B; 1 mm in C,D; 50 μm in E; 100 μm in F.

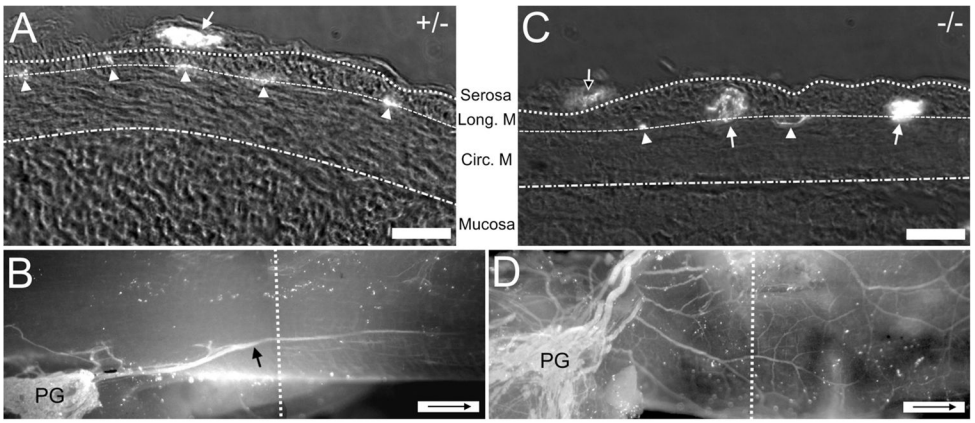

Figure 3.

Comparison of the location of nerve fibers with respect to the wall of the colon in Ednrb$^{+/-}$ and *Ednrb*$^{-/-}$ preparations. **A**: Cross-section of P9 Ednrb$^{+/-}$ colon. Fluorescence indicates the presence of neurofilament-IR (bright spots, NF). Arrow indicates large sacral fascicle superficial to longitudinal muscle. Arrowhead shows fibers within the muscle layers indicating the location of the myenteric plexus. **B**: A montage showing a whole-mount view of the colon sectioned in (A). An extrinsic sacral fiber (arrow) arises from the pelvic ganglia (PG). The dotted line indicates the approximate area where the cross-section was cut. **C**: Cross-section of P9 *Ednrb*$^{-/-}$ colon. Large NF+ sacral fiber bundles (arrows) and smaller fiber bundles (arrowheads) are located between the muscle layers except for one small fascicle (open arrow) on the surface of the longitudinal muscle. **D**: A montage showing a whole-mount view of the colon sectioned in (C). Multiple fiber bundles are present although ganglia are not. The dotted line shows the position where section (C) was cut. Arrow inside scale bar indicates oral direction. Scale bars = 30 μm in A,C; 500 μm in B,D.

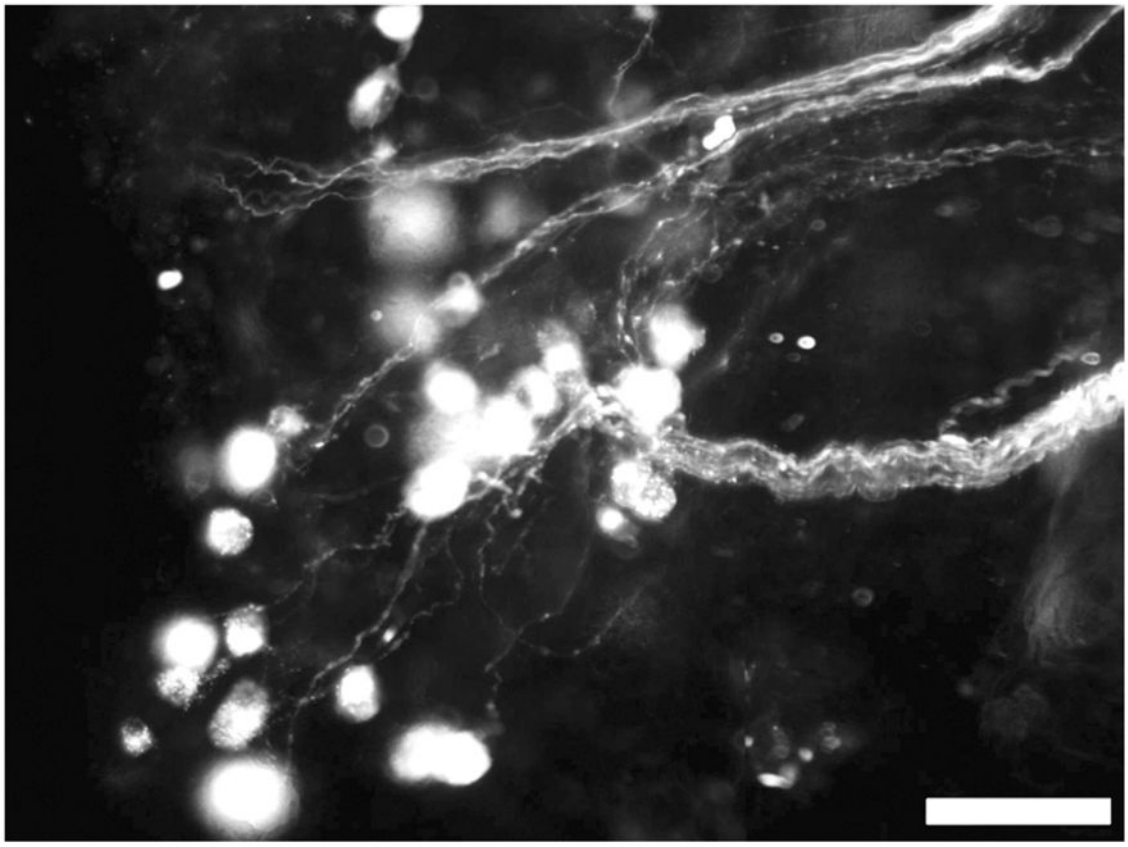

Figure 4.
Cells in the pelvic ganglion from a P29 *Ednrb*$^{-/-}$ mouse are fluorescent after application of DiI crystals to nerve fibers in the mid-colon. Scale bar = 50 μm.

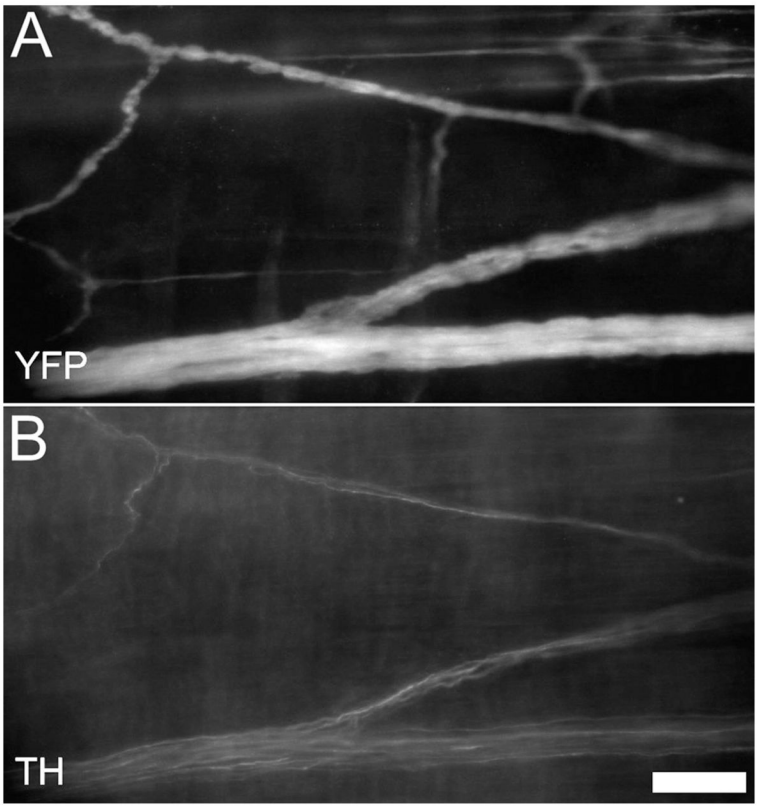

Figure 5.
P17 Sacral nerve fibers. Some of YFP+ sacral fibers (**A**) are immunoreactive for tyrosine hydroxylase (**B**, TH). Scale bar = 50 μm.

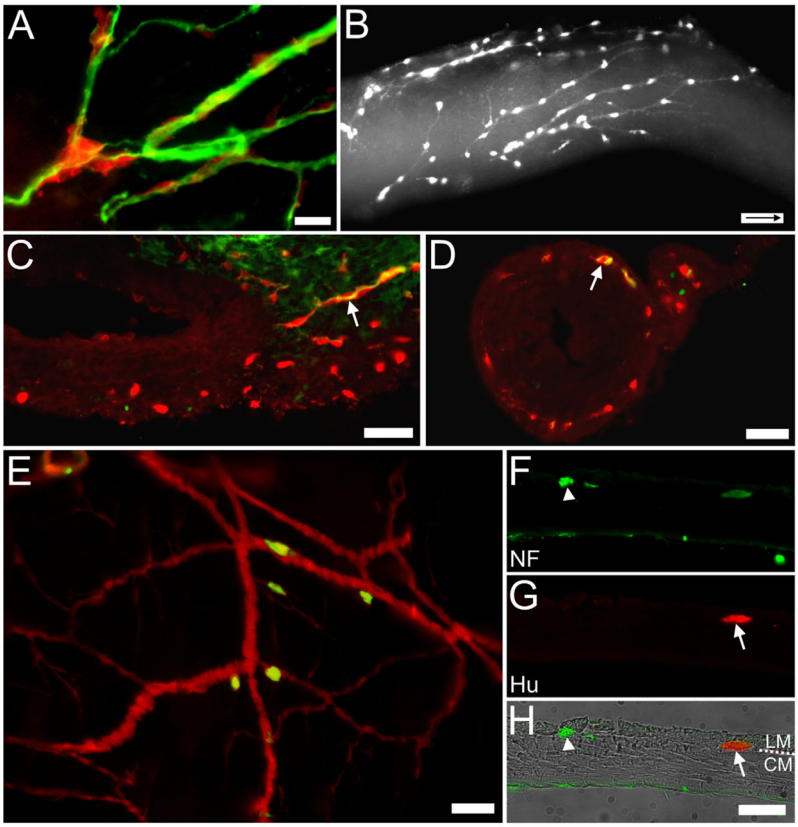

Figure 6.

Cells on nerve fibers in *Ednrb*$^{-/-}$ preparations. **A**: Surface view. E14.5 YFP+ SNCCs (red) appear along βIII-tubulin-immunoreactive nerve fibers (green) within the distal colon. **B**: Surface view. E15.5 YFP+ cells are found along nerve fibers in the distal colon heading in an oral direction (arrow inside scale bar indicates oral direction). **C**: Section through another E15.5 distal colon just oral to the pelvic ganglion. A βlll-tubulin-immunoreactive fiber (green) and YFP+ cells (red) together enter the wall of the colon where many YFP+ cells are already present. **D**: Section through the E15.5 distal colon in a position more oral than (C). A YFP+ cell (red) and βlll-tubulin-immunoreactive fibers (green) are colocalized (arrow); numerous YFP+ cells are found between the muscle layers. **E**: Whole mount of P7 distal colon. Hu+ (green) cells are found on YFP+ (red) nerve fibers near the pelvic ganglia. **F–H**: Cross-section of P31 distal colon. (F) Both a faintly stained YFP+ cell and neurofilament-immunoreactive nerve fibers (green, arrowhead) are located between the muscle layers while nerve fibers are also found at the edge of the muscle-submucosa interface. The submucosa and the mucosa were removed. (G) An Hu+ (red) neuron is found between the muscle layers usually occupied by the myenteric ganglia. (H) Overlay of images with brightfield image and the circular (CM) and longitudinal muscles (LM) labeled. Scale bars = 50 μm in A,C–H; 100 μm in B. A magenta-green copy of this figure is available as Supporting Figure 3.

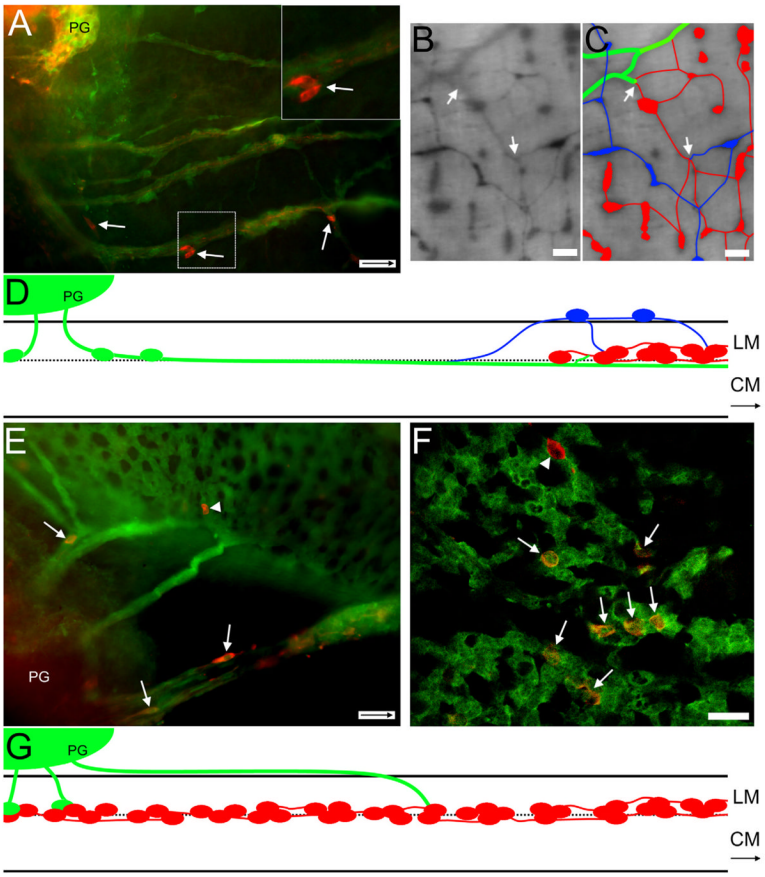

Figure 7.

A: E16.5 *Ednrb*$^{-/-}$. TH+ cells (arrows) and fibers accompany sacral fibers projecting orally from the PG into the colon. Note the absence of ganglia. Inset, upper right: Two TH+ cells within box are shown at higher magnification. **B**: P27 *Ednrb*$^{-/-}$. Changes in position of extrinsic fibers when encountering intrinsic ganglia. Neural crest-derived cells are labeled with β-galactosidase. Cells and fibers on the serosal surface are sharp and dark while cells and fibers within the muscle layers are lighter and blurry. **C**: Overlay of fibers shown in (B). At the site where the sacral fibers extend into the region of vagal ganglia in the midcolon, large sacral fibers (green) are located between the muscle layers, the same level as vagal ganglia (red). There are also ganglia in the serosal region (blue), above the vagal ganglia, whose origin could be either cells that traveled from sacral axons and/or from the vagally derived intrinsic neurons in the hypoganglionic region. These different elements appear to intersect (arrows). **D**: Diagram summarizing the findings for *Ednrb*$^{-/-}$ aganglionic colon. Sacral extrinsic fibers and cells (green) projecting from the pelvic ganglia (PG) intersect with the vagal myenteric plexus (red) in the mid-colon. A population of cells and smaller fascicles (blue) appear at the vagal wavefront. They exit the myenteric locale and reside in the serosal region superficial to the longitudinal muscle (LM) where they appear to have connections with vagal ganglia. The larger sacral fascicles continue orally between the muscle layers where they appear to intermingle with the vagal ganglia. CM: circular muscle. **E**: *Ednrb*$^{+/-}$. YFP+ sacral fibers (green) extending from the pelvic ganglia (PG) into the distal colon contain TH+ cells (red, arrows). A single TH+ cell (arrowhead) is incorporated into ganglia formed by VNCCs. **F**: E16.5 *Ednrb*$^{+/-}$ colon. A confocal image showing TH+ (red, arrows) YFP+ SNCCs among the YFP+ VNCCs (green) forming nascent ganglia. Note a single TH+ cell that is not YFP+ (arrowhead). **G**: Diagram summarizing the findings for

Ednrb$^{+/-}$ ganglionated colon. Fibers leaving the pelvic ganglion travel the longest distance superficial to the longitudinal muscle before penetrating the muscle and terminating between the muscle layers. SNCC (green) cells move along extrinsic fibers to reach VNCC myenteric ganglia (red) where they become incorporated into the ganglia. Arrows inside scale bar indicate oral direction. Scale bars = 50 μm in A,E; 250 μm in B,C; 25 μm in F; D,G not to scale. A magenta-green copy of this figure is available as Supporting Figure 4.

TABLE 1

Primary Antibodies

Antigen	Immunogen	Manufacturer, species antibody was raised in, mono-vs. polyclonal, catalog no.	Dilution
GFP (green fluorescent protein)	Purified GFP	Abcam, Rabbit polyclonal, AB290	1/500
GFP	Purified recombinant GFP	Aves Labs (Tigard, OR), Chicken polyclonal, GFP-1020	1/1,000
Hu (human neuronal protein)	Hu protein. Immunoblot recognizes only 41kDa neuronal protein	Serum obtained from patient (Madison, WI), Fairman et al., 1995, Human	1/1,000
β III tubulin (TuJ1)	Peptide EAQGPK corresponding to the C-terminus of β III tubulin	Dr. A. Frankfurter, Mouse monoclonal	1/1,000
NF (neurofilament)	Rat m-neurofilament protein containing the C-terminus 168AA fused to *E. Coli* Trp-E	Chemicon (Temecula, CA), Rabbit polyclonal, AB1987	1/200
TH (tyrosine hydroxylase)	TH purified from PC12 cells	IncStar (Minneapolis, MN), Mouse monoclonal, 22941	1/1,000
TH	A mixture of two different anti-peptide antibodies corresponding to human and mouse residues. One was generated against a peptide near the N-terminus: RRQ SLI EDA RKE RE and the other near the C-terminus of TH: SDA KDK LR[N/S] YAS RIQ R	Aves Labs (Tigard, OR), Chicken polyclonal, TYH	1/1,000
NOS (nitric oxide synthase)	AA1095-1289 of human NOS	BD Transduction Labs, Rabbit polyclonal, N31030/L15	1/200
NOS	Rat recombinant NOS	Gift from PC Emson (Cambridge, UK), Sheep polyclonal	1/2,000
VIP (vasoactive intestinal polypeptide)	Porcine VIP-coupled to thyroglobulin	Epstein and Paulsen 1991 (Madison, WI), Rabbit polyclonal	1/500

TABLE 2

Secondary Antibodies

Name	Conjugated to	Manufacturer, catalog no.	Dilution
Donkey antichick	Cy2	Jackson ImmunoResearch, 703-225-155	1/1,000
Donkey antichick	Cy3	Jackson ImmunoResearch, 703-165-155	1/1500
Donkey antichick	Dylight 549	Jackson ImmunoResearch, 703-505-155	1/1,000–1/1,250
Donkey antirabbit	Dylight 488	Jackson ImmunoResearch, 711-485-152	1/500
Donkey antihuman	Dylight 488	Jackson ImmunoResearch, 709-485-149	1/1,000
Goat antimouse	Cy3	Jackson ImmunoResearch, 115-505-003	1/1,500
Donkey antisheep	Cy3	Jackson ImmunoResearch, 713-165-147	1/1,500